References

[1] R. G. Plumb, R. F. Harrington, and A. T. Adams, "An electromagnetic model for multiconductor connectors," *IEEE Trans. Electromagn. Compat.*, vol. 32, pp. 38–52, Feb. 1990.

[2] R. G. Plumb and R. F. Harrington, "The electromagnetic response of a multiconductor connector," Report TR-88-15, Syracuse Univ., Syracuse, NY, 1988.

[3] C. R. Paul, "Useful matrix chain parameter identities for the analysis of multiconductor transmission lines," *IEEE Trans. Microwave Theory Tech.*, vol. MTT-23, pp. 756–760, Sept. 1975.

[4] N. Balabanian and T. Bickart, *Linear Network Theory*. Beaverton, OR: Matrix, 1981.

Full-Wave Analysis of Multilayer Coplanar Lines

Chia-Nan Chang, Wen-Chang Chang, and Chun Hsiung Chen

Abstract—**A full-wave analysis of a coplanar wave-guiding structure with multiple dielectric layers is presented. In this study, the results of the hybrid approach that combines the finite-element method and the conformal-mapping technique are compared with those of the spectral-domain approach. Numerical results for effective dielectric constants, characteristic impedances, current distributions, and field distributions for various multilayer coplanar line structures are presented and discussed. Comparisons are also made of the computed results with the available quasi-static ones.**

I. Introduction

With the increased use of suspended substrate lines and for special purposes such as protection from mechanical or chemical damage and the provision of additional means to adjust the transmission line characteristics, the study of multilayer planar wave-guiding structures has received the attention of a number of investigators [1]–[5]. Instead of analyzing the problem directly in the space domain, most previous work has been carried out in the spectral domain. Rapidity in obtaining the dispersion characteristics of the lines is an advantage of this technique. However, it is not so easy to obtain both the field patterns and the characteristic impedances of multilayer planar wave-guiding structures because of the complicated mathematical manipulation of the fields from the spectral domain to the space domain.

In a recent investigation, a rigorous hybrid full-wave analysis of coplanar waveguide is presented [6]. In that work, the infinite space in the original domain is first mapped into a finite region in the image domain by the mapping function originally employed by Wen [7]. The transformed variational equation in the image domain is then solved efficiently by the conventional finite-element method. In this way, the difficulties associated with both the infinite space and the field singularity near the conductor edges can be removed. In this paper, the same hybrid approach is utilized to study the full-wave characteristics of a coplanar line structure with multiple dielectric layers. Especially, the frequency-dependent effective dielectric constants and characteristic impedances of the multilayer coplanar line are calculated and compared with available data [4], [5]. Also investigated are the field distribution along the center line of the slot and the current distributions on both the signal strip and the ground plane. Because of a lack of data for comparison, the results of this hybrid approach are validated by a comparison with those of the spectral-domain approach [5].

Manuscript received May 17, 1990; revised November 5, 1990. This work was supported by the National Science Council, Republic of China, under Grant NSC 79-0404-E002-39.

The authors are with the Department of Electrical Engineering, National Taiwan University, Taipei 10764, Taiwan, Republic of China.

IEEE Log Number 9042503.

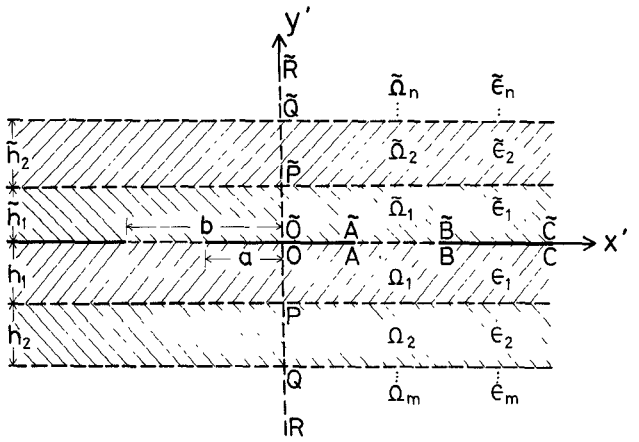

Fig. 1. Geometry of mulilayer coplanar line and original domain ($x' \geq 0$) in z' plane.

II. Formulation

Consider an open uniform coplanar line structure with multiple layers of isotropic and lossless dielectrics as shown in Fig. 1. Here a central metal strip (assuming negligible thickness) of width $2a$ and two conducting ground planes (also of negligible thickness) of separation $2b$ are placed in the plane ($y'=0$) between dielectric layers. Above and below the conductors are n upper and m lower homogeneous dielectric layers of permittivities $\tilde{\epsilon}_k = \epsilon_0 \tilde{\epsilon}_{rk}$ ($k=1,2,\cdots,n$) and $\epsilon_k = \epsilon_0 \epsilon_{rk}$ ($k=1,2,\cdots,m$), respectively. The guided modes of this inhomogeneous structure are in general hybrid; therefore, both the axial components E_z and H_z are required in the analysis. As far as the fundamental (E_z even and H_z odd) mode is concerned, it is sufficient to consider the right half structure with a magnetic wall at $x'=0$.

A. Hybrid (Finite-Element / Conformal-Mapping) Approach

Following the idea of [6], Wen's mapping function [7]

$$z' = a\,\mathrm{sn}(z,k) \tag{1}$$

is used to map the right half plane $x' \geq 0$ (original domain) in Fig. 1 into a rectangular region (of width $2K(k)$ and height $K(k')$) in the image domain (Fig. 2). Here, $\mathrm{sn}(z,k)$ is the complex sine elliptic function, $K(k)$ and $K(k')$ are the complete elliptic integrals of the first kind and the second kind [8], $k = a/b$, and $k' = \sqrt{1-k^2}$. By this mapping, the transverse fields $(\vec{E}_t, \vec{H}_t)$ are smooth everywhere in the image domain [6], although the transverse fields $(\vec{E}_t', \vec{H}_t')$ in the original domain exhibit edge singularity near the conductor edges. Thus the field singularity difficulty in the original domain may be removed.

The variational formulation for the multilayer coplanar lines in the image domain (Fig. 1) is the same as [6, eq. (1)], and the boundary conditions on the electric and magnetic walls are shown in Fig. 2. The details of the numerical procedures are given in [6].

B. Spectral-Domain Approach

For purposes of cross checking, the new type of spectral-domain approach [9] is also applied to the multilayer coplanar

0018-9480/91/0400-0747$01.00 ©1991 IEEE

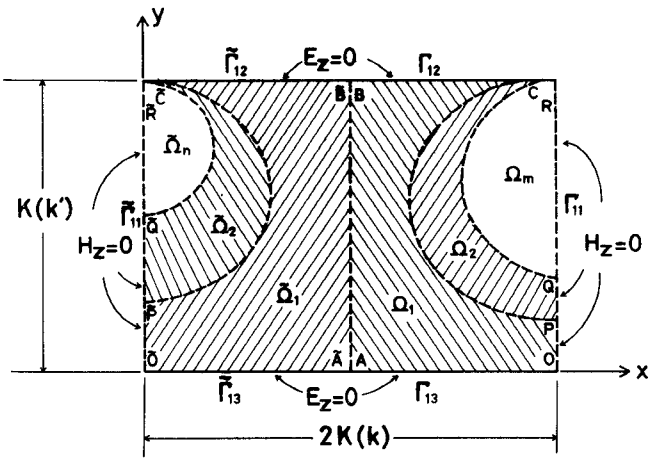

Fig. 2. Corresponding image domain in z plane and boundary conditions.

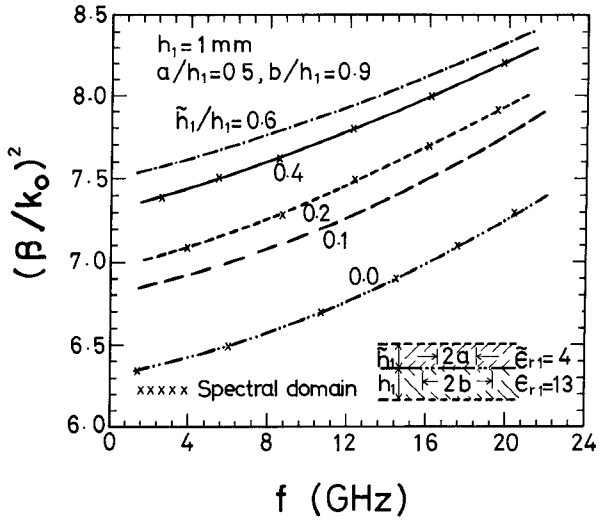

Fig. 3. Effective dielectric constant versus frequency with $\tilde{h}_1/h_1$ as parameters (comparison with results of spectral-domain method).

line (Fig. 1), giving an equation of the form

$$\begin{bmatrix} \tilde{G}_{xx} & \tilde{G}_{xz} \\ \tilde{G}_{zx} & \tilde{G}_{zz} \end{bmatrix}^{-1} \begin{bmatrix} \tilde{E}_x \\ \tilde{E}_z \end{bmatrix} = \begin{bmatrix} \tilde{J}_x \\ \tilde{J}_z \end{bmatrix}. \tag{2}$$

Here, $\tilde{E}_x$, $\tilde{E}_z$, $\tilde{J}_x$, and $\tilde{J}_z$ denote the Fourier transforms of the x and z components of the electric field and the current density, respectively, while $\tilde{G}_{ij}$ (i, $j=x$ or z) represent the Fourier transforms of the associated Green's functions. The Green's functions $\tilde{G}_{ij}$ in the spectral domain are determined by the transmission-line technique given by Das and Pozar [3]. The longitudinal component E_z is small compared with the transverse one, E_x, as suggested by the hybrid approach in [6]; hence $\tilde{E}_z$ is neglected in (2) and only $\tilde{E}_x$ is treated by the Galerkin method. For a representation of the unknown slot field E_x, the expansion functions proposed by [9] are adopted in this investigation.

III. Numerical Results and Discussions

A. Effective Dielectric Constants

In Fig. 3, the frequency-dependent effective dielectric constants, from the hybrid approach, for the two-layer coplanar line are presented. Also shown, for comparison, are the results of

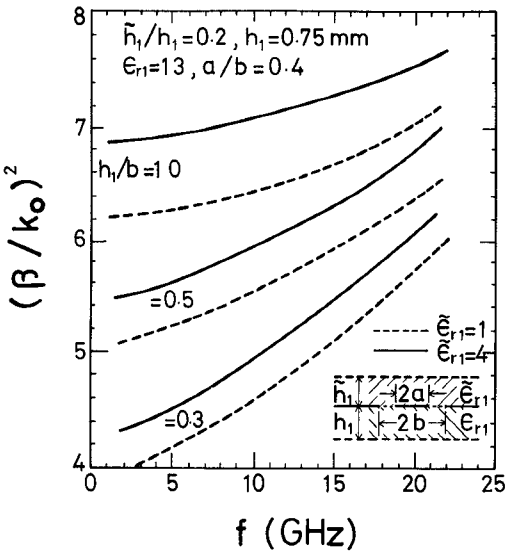

Fig. 4. Effective dielectric constant versus frequency with h_1/b as parameters.

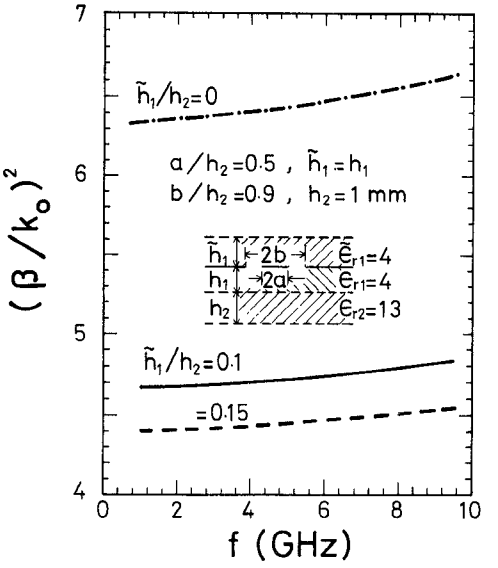

Fig. 5. Effective dielectric constant versus frequency with $\tilde{h}_1/h_2$ as parameters.

the spectral-domain approach. Excellent agreement is observed, which confirms the accuracy of the two methods. It is noted that the increase of the effective dielectric constant is not negligible, even with the insertion of a thin dielectric film above the metallic electrodes.

The dispersive effective dielectric constants are shown in Fig. 4, with h_1/b as parameters. In this figure, larger values of h_1/b correspond to narrower widths of both signal strip and slot. The nearly parallel curves for various h_1/b values indicate little influence of an upper dielectric layer on the frequency-dependent behavior of the waveguide.

In Fig. 5, the effects of inserting two dielectric films, one on the top and the other on the bottom of metallic electrodes, are presented. The addition of a lower dielectric film between the metallic electrodes and the substrate causes a decrease of effective dielectric constants, while the addition of an upper film causes an increase. Note that the modification of effective dielectric constants is not negligible, even with the insertion of a

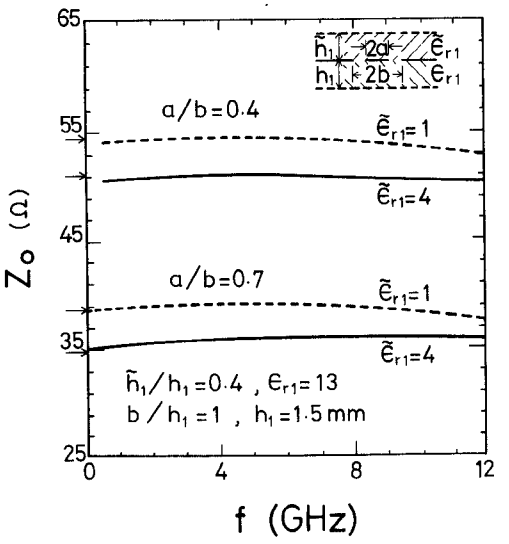

Fig. 6. Characteristic impedance Z_0 versus frequency with both a/b and $\tilde{\epsilon}_{r1}$ as parameters (comparison with results of quasi-static analysis).

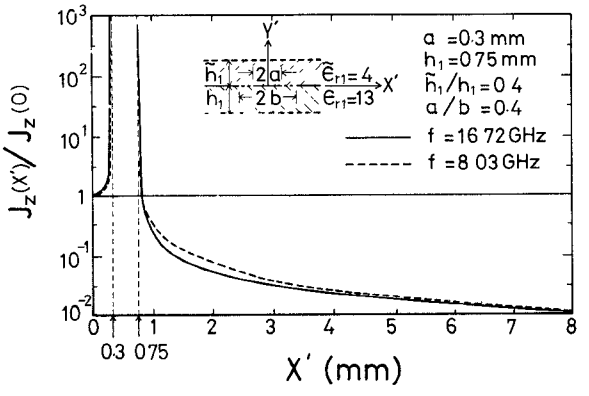

Fig. 7. Normalized current distributions on both signal strip and ground plane with frequencies as parameters.

thin dielectric film below the metallic electrodes. Note also that the impact of the lower dielectric film on the effective dielectric constant is stronger than that of the upper dielectric film of equal dielectric constant and equal thickness, as can be seen in Fig. 5, where both thicknesses are varied simultaneously.

B. Characteristic Impedances

Shown in Fig. 6 are the frequency-dependent characteristic impedances with both a/b and $\tilde{\epsilon}_{r_1}$ as parameters. Here the characteristic impedance is calculated based on the voltage–current definition: $Z_0 = V_s/I_{zl}$, where V_s denotes the voltage defined along the interface of ϵ_{r1} and $\tilde{\epsilon}_{r1}$, and I_{zl} is the total longitudinal current on the signal strip [6]. Since the integration region is finite and the fields are nonsingular in the image domain, we calculate both quantities in this domain. The increase in strip width causes an increase of line capacitance in the quasi-static approximation; hence a decrease in characteristic impedance is observed in this figure. The insertion of an upper dielectric layer on top of the metallic electrodes causes an increase in the effective dielectric constant and hence also a decrease in the characteristic impedance of the waveguide.

The arrows in the left hand side of Fig. 6 indicate the calculated results of the quasi-static analysis [4]. Agreement of the results is observed, with a maximum deviation of 1.5%. The small variation of the four curves in this figure implies the validity of the quasi-static analysis at this lower frequency range of operation.

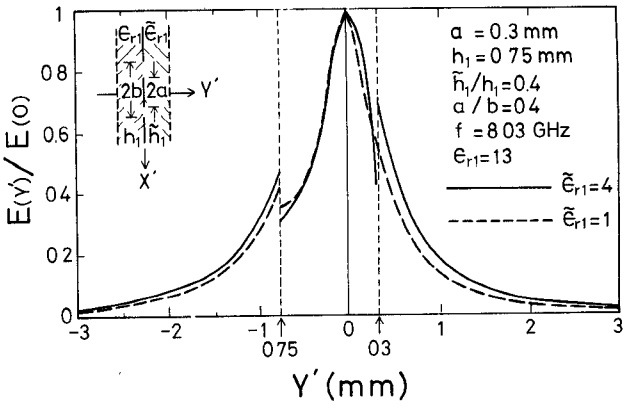

Fig. 8. Distributions of total electric field along the line $x' = 0.5(a+b)$ with $\tilde{\epsilon}_{r1}$ as parameters.

C. Current Distributions

In Fig. 7, the normalized longitudinal current distributions $J_z(x')/J_z(0)$ on both the signal strip and the ground plane are plotted on a logarithmic scale. As expected, the longitudinal currents exhibit the edge singularity at points near the conductor edges. Note that a greater increase of the longitudinal current occurs at the signal strip edge than that at the ground plane edge. Note also the decay of the longitudinal current away from the ground plane edge. This decay information is useful in designing the finite-extent ground planes in practice. The calculated order of J_x/J_z on the conductor strip is observed to be less than 3%.

D. Field Distributions

The calculated normalized transverse field distributions $E_x/E_{x_{min}}$ over the slot exhibit the same edge singularity as those of [6, fig. 6] and are not presented here. The nearly frequency-independent and symmetric distribution of such a normalized transverse field distribution supports the essential assumption in the spectral-domain analysis of multilayer coplanar lines [5]. The ratio E_z/E_x at any point over the slot is observed to be smaller than 0.02, which makes the zero longitudinal field assumption in the spectral-domain analysis acceptable.

Shown in Fig. 8 are the normalized total electric field distributions along the line $x' = 0.5(a+b)$ of the multilayer coplanar line. As a result of the continuous normal electric flux density, the field just near the interface of the smaller permittivity region is stronger than that in the larger permittivity region. The total electric field is confined along the y' axis, as expected, but the field confinement is not improved by the insertion of an upper dielectric layer.

IV. Conclusions

A full-wave analysis of multilayer coplanar lines, based on hybrid and spectral-domain approaches, has been presented. Numerical results for effective dielectric constants, characteristic impedances, current distributions, and field distributions have been computed and compared with available ones, and good agreement has been obtained.

References

[1] J. B. Davis and D. Mirshekar-Syahkal, "Spectral domain solution of arbitrary coplanar transmission line with multilayer substrates," *IEEE Trans. Microwave Theory Tech.*, vol. MTT-25, pp. 143–146, Feb. 1977.

[2] T. Itoh, "Spectral domain immittance approach for dispersion characteristics of generalized printed transmission lines," *IEEE Trans. Microwave Theory Tech.*, vol. MTT-28, pp. 733–736, July 1980.

[3] N. K. Das and D. M. Pozar, "A generalized spectral-domain Green's function for multilayer dielectric substrates with application to multilayer transmission lines," *IEEE Trans. Microwave Theory Tech.*, vol. MTT-25, pp. 326–335, Mar. 1987.

[4] C. N. Chang, "Analysis of coplanar waveguiding structures," Ph.D. dissertation, Graduate Institute of Electrical Engineering, National Taiwan University, July 1990.

[5] W. C. Chang, "Spectral-domain analysis of planar waveguides," Master's thesis, Graduate Institute of Electrical Engineering, National Taiwan University, July 1990.

[6] C. N. Chang, Y. C. Wong, and C. H. Chen, "Full-wave analysis of coplanar waveguides by variational conformal mapping technique," *IEEE Trans. Microwave Theory Tech.*, vol. 38, pp. 1339–1344, Sept. 1990.

[7] C. P. Wen, "Coplanar waveguide: A surface strip transmission line suitable for nonreciprocal gyromagnetic device applications," *IEEE Trans. Microwave Theory Tech.*, vol. MTT-17, pp. 1087–1090, Dec. 1969.

[8] I. S. Gradshteyn and I. M. Ryzhik, *Table of Integrals, Series, and Products*. New York: Academic Press, 1965.

[9] K. Uchida, T. Noda, and T. Matsunaga, "New type of spectral-domain analysis of a microstrip line," *IEEE Trans. Microwave Theory Tech.*, vol. 37, pp. 947–952, June 1989.